Tellus SERIES B CHEMICAL AND PHYSICAL METEOROLOGY
PUBLISHED BY THE INTERNATIONAL METEOROLOGICAL INSTITUTE IN STOCKHOLM

Tellus (2011), 63B, 959–970

TELLUS

Distinguishing the provenance of fine-grained eolian dust over the Chinese Loess Plateau from a modelling perspective

By ZHENGGUO SHI[1]* and XIAODONG LIU[1,2], [1]*State Key Laboratory of Loess and Quaternary Geology, Institute of Earth Environment, Chinese Academy of Sciences, Xi'an, China;* [2]*Department of Environmental Science and Technology, School of Human Settlements and Civil Engineering, Xi'an Jiaotong University, Xi'an, China*

(Manuscript received 1 December 2010; in final form 29 May 2011)

ABSTRACT

The provenance of fine-grained eolian dust over East Asia is distinguished using a regional climate model. Five major source regions within China and Mongolia are considered: sandy lands in the northeastern China, deserts in the northern China, the Gobi deserts, the Taklimakan deserts in western China and deserts on the Tibet an Plateau. The contribution of each dust source is evaluated for the downwind eolian sediments in the Chinese Loess Plateau (CLP) and Japan Sea (JS). The results show that the adjoining northern and Gobi deserts dominate the dust depositions over CLP and over eastern China, although Taklimakan deserts are actually the largest emission source. On the marine deposits in JS, Taklimakan deserts exert a more significant role since the particles from Taklimakan tend to be raised into upper atmosphere and delivered for a longer distance. The agent for dust delivery also differs among different sources. Dust from northern deserts is dominantly carried by the local northwesterly winds in spring associated with the East Asian winter monsoon system and restricted in the low-level atmosphere, while the westerly winds in the mid- to high-level troposphere become of great importance and more likely to be responsible for the transport of Taklimakan dust.

1. Introduction

Dust aerosols, which mainly originate from the arid/semi-arid regions, have significant influences on climate by modifying the radiation budget and cloud-precipitation physics (e.g. Tegen and Lacis, 1996; Miller et al., 2004; Rosenfeld, 2000), and also by providing nutrients for terrestrial and aquatic organisms and impacting the biogeochemical cycles (Duce et al., 1991). As one of the main contributors of global dust loading, Asian dust cannot only remarkably affect the regional climate but also induce significant adverse effects on human health in East Asia. Due to its particular significance, the variability of Asian dust on different timescales and its climatic feedbacks have received much attention over the years (e.g. Gong et al., 2006; Porter and An, 1995; Zhang et al., 2009).

Dust deposits have been used as proxies of past environmental changes. Actually, dust concentrations in ice cores and marine sediments vary nearly synchronously with the past climate variations, for example, the temperature and the atmospheric CO_2 concentration (Delmonte et al., 2002; Lambert et al., 2008). Of great interest is the Chinese Loess Plateau (CLP), located at the downwind regions of the Asian deserts, which is a unique region on earth that its geological history has significant implications to the understanding of the paleoenvironment. The CLP is widely accepted to be formed by a thick deposition of eolian dust blanketing the underlying topography (Liu, 1985). The loess sections can provide unique continuous high-resolution records for East Asian monsoon intensity during the past several million years (An, 2000). The knowledge on the Asian dust sources and the associated circulation patterns, and the contributions of different sources to the total Asian dust loading and eolian deposits, especially over the CLP, will help to determine how much about the past climate change we can extract from the loess records.

To distinguish the provenance of the Chinese loess, various geochemical tracers have been extensively explored. For example, widely used tracers of eolian dust transport include the elemental ratios of Fe/Al, Mg/Al and Sc/Al (Zhang et al., 1996), oxygen isotopes (Chung et al., 2003; Hou et al., 2003) and electron spin resonance signals (Sun et al., 2008) of quartz, strontium and neodymium isotopes (Biscaye et al., 1997; Sun,

*Corresponding author.
e-mail: shizg@ieecas.cn
DOI: 10.1111/j.1600-0889.2011.00561.x

2002; Nakano et al., 2004), and soil carbonate contents (Wang et al., 2005; Cao et al., 2005). The deserts in the western and northern China and the Gobi deserts in Mongolia are considered as three major sources of eolian deposits of the CLP (Sun et al., 2001). However, the exact sources of loess and the relative importance of each source are still unclear, with debates on whether Taklimakan desert is one of the primary sources (Liu et al., 1994; Torii et al., 2001; Zhang et al., 1996) or not (Sun, 2002; Sun et al., 2008). In addition, the Tibetan Plateau might also play a significant role in producing eolian deposits for the surrounding regions to its east (Fang et al., 2004).

Another focus is on the transport mechanisms and pathways of Chinese eolian dust. The East Asian winter monsoon and westerly are usually considered as two candidates for dust delivery (Sun, 2004). It is generally hypothesized that the coarse component is entrained mainly by low-altitude winds of winter monsoon circulation, and most part of the fine component is transported by high-altitude westerly. Tracer studies can provide useful constraints for determining the provenance of eolian dust from observation sites. However, limited soil samples can not be expected to completely represent the entire region, in which the observation sites are located, since the soil characteristics change significantly even on a very small spatial scale. Hence, it is extremely difficult for observational studies to directly determine exactly where the eolian dust comes from at particular sites; in most cases, they can merely show the consistencies in certain properties between the soil samples from the dust sources and deposition sites.

Numerical studies can well reproduce the basic processes of eolian dust cycles, including the emission, transport and deposition, and thus provide necessary insights for the provenance of eolian dust in particular regions from a more physical perspective. Till now, several modelling studies have been undertaken to reproduce the distribution of dust aerosol and to distinguish the provenance of eolian deposits on the global scale (e.g. Luo et al., 2003; Tanaka and Chiba, 2006; Li et al., 2008). Some observational studies point out that the eolian deposits from CLP and North Pacific are dominated by the dust from the inner Asian deserts (Sun and An, 2002; Rea et al., 1998), but it is still controversial whether dust in Greenland ice cores originates from Asian deserts (Biscaye et al., 1997; Bory et al., 2003). Although the eolian dust in the near-source CLP is considered to be dominantly from deserts in China and Mongolia both in modern time and the last glacial maximum (Sun et al., 2008), it is still an open question which deserts are mainly responsible for the eolian deposits in the CLP.

In this study, a high-resolution regional climate model is employed to distinguish the provenance of the fine-grained eolian dust in the CLP by conducting a series of experiments. The deposition flux in the Japan Sea (JS) is also examined for comparison. The main objectives include distinguishing the major source regions within China and Mongolia, which supply eolian dust to the CLP and entire East Asia, and quantifying the respective contribution from each source. The model and experimental design are described in Section 2. In Section 3, we analysed our simulated results, particularly the relative contributions of different sources to the column dust loading and deposition flux. Finally the main conclusions are presented in Section 4.

2. Numerical model and experimental design

2.1. Numerical model

The model used in this study is the Regional Climate Model RegCM version 3 (RegCM3) developed by the Abdus Salam International Centre for Theoretical Physics (ICTP) (Pal et al., 2007). It has been proved to be able to well reproduce the climate and dust cycle in East Asia in previous studies (Zhang et al., 2009). RegCM3 is a hydrostatic, sigma vertical coordinate model whose dynamical framework is essentially the same as the mesoscale model MM5. The solar and atmospheric radiation budgets are calculated based on the scheme of Kiehl et al. (1996). The boundary layer processes are described by the non-local parameterization of Holtslag et al. (1990). Land surface processes, represented via the Biosphere–Atmosphere Transfer Scheme (BATS) (Dickinson et al., 1993), provide most of the variables used to couple the dust emission scheme. The moisture convection and non-convective precipitation are respectively parameterized by Grell (1993) and Pal et al. (2000).

The dust scheme coupled on-line is described in detail by Zakey et al. (2006), which generally include the emission, transport and deposition processes of dust particles. The dust production is following Marticorena and Bergametti (1995) and Alfaro and Gomes (2001), which is represented as a function of wind conditions, soil surface characteristics and particle size. It is generally recognized that dust particles are mobilized only if wind speed is greater than a threshold value and the threshold friction velocity is associated with surface roughness (Marticorena and Bergametti, 1995) and soil moisture (Fecan et al., 1999). The horizontal mass flux is calculated as a function of the critical friction velocity and then the vertical flux corresponding to each emission mode is obtained. These calculations become effective only if the model grid cell is covered by desert and semi-desert in the BATS interface while sub-grid fractional desert surface has not been accounted for in this study. This means that a grid cell is classified entirely either as desert or as non-desert. The size spectrum of the dust module covers particles from 0.01 to 20.0 μm in diameter and is divided into four transportable bins: the fine (0.01–1.0 μm), accumulation (1.0–2.5 μm), coarse (2.5–5.0 μm) and the giant (5.0–20.0 μm) modes. The transport processes are parameterized by the tracer transport equation of Solmon et al. (2006) and Zakey et al. (2006), which includes transport by resolvable scale winds, sub-grid scale turbulences and deep convection, gravitational settling, and wet and dry removal processes. Wet deposition is treated following Giorgi (1989) for resolvable scale precipitation and Giorgi and

Chameides (1986) for convective precipitation. The size-dependent particle gravitational settling and dry deposition terms are described by Zakey et al. (2006). And the dust mass accumulation rate (MAR) is calculated in this study as the sum of wet and dry deposition fluxes.

2.2. *Experimental design*

In our simulations, the model domain covers the northern China and Mongolia with a spatial resolution of 50 km (Fig. 1), which includes the entire arid/semi-arid regions in East Asia. The model is run at its standard configuration of 18 vertical sigma layers and model top at 50 hPa. The weekly sea surface temperature data are from the National Oceanic and Atmospheric Administration (NOAA) Optimum Interpolation Sea Surface Temperature (OISST) data set (Reynolds et al., 2002) and the meteorological initial and time-evolving lateral boundary conditions for RegCM3 are obtained from the National Centre for Environmental Prediction (NCEP) reanalysis (Kalnay et al., 1996). No chemical boundary condition is included so that all aerosols from sources out of model domain are neglected in our study. The default land use types from the Global Land Cover Characterization (GLCC) data (Loveland et al., 2000) within China are modified based on the WESTDC Land Cover Products (provided by the Environmental and Ecological Science Data Center for West China, National Natural Science Foundation of China, available at http://westdc.westgis.ac.cn), in order to specify the sandy regions (e.g. Horqin, Onqin Daga) in the northeastern China. Outside China, the land use types are kept unchanged. The corresponding soil texture data are also modified for extra dust sources following Hseung (1996). Although debates exist on whether or not there are deserts on the western Tibetan Plateau between these two data sets, we follow the GLCC data to include all possible dust sources in this region.

For our purpose, the primary desert areas are divided into five potential source regions (Fig. 1): (A) Horqin and Onqin Daga deserts in the northeastern China; (B) Badain Juran, Tengger and Mu Us deserts close to CLP in northern China; (C) Gobi deserts in Mongolia; (D) Taklimakan and Gurbantnggut deserts and (E) the western Tibet and Kumtag deserts. These source regions are respectively named, hereafter, as the northeastern sandy lands, near-CLP northern deserts, Gobi, Taklimakan and Tibetan deserts. Two depositional regions are considered, one is the CLP (105–115°E, 33–37°N) and the other is the remoter Japan Sea (JS, 130-138°E, 38–42°N) for comparison. Six experiments (abbreviated as All, NoA, NoB, . . ., NoE for experiments with all deserts and without the source region A, B, C, D and E, respectively) are performed in total using different landuse maps to turn off the dust emissions of different source regions, extending from November 1993 to February 1999. In order to compare with geological periods, our focus is mainly to analyse the natural dust cycle under modern climate conditions. Thus, the anthropogenic aerosols, for example, black carbon and sulfate, are neglected in our study although they could mix with the dust particles and significantly affect their life cycles and properties (Clarke et al., 2004). The radiative feedback from dust aerosols is also not considered. The results of the last 5 years (March 1994–February 1999) are analysed and averaged as the mean state of the modern dust cycle.

The percentage contribution of a given source region 'X' to a dust-related element 'F' (C_{FX}) is calculated as follows:

$$C_{FX} = (F_{All} - F_{NoX}) \Big/ \sum (F_{All} - F_{NoX}) \quad (X = A, B, \ldots, E)$$

in which, F_{All} is the results of simulations with all deserts and F_{NoX} is the simulation results with the source region 'X'

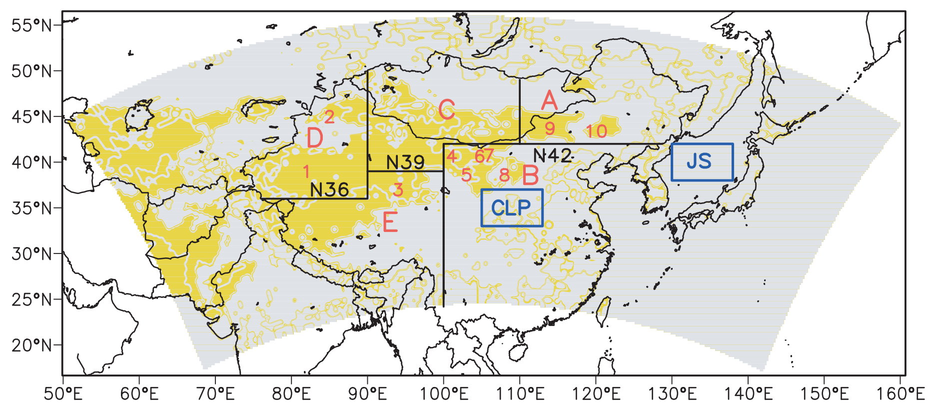

Fig. 1. Model domain in this study. Also shown is the dust source regions (yellow shaded) and ten Chinese deserts: 1. Taklimakan (Area: 337600 km^2), 2. Gurbantunggut (48800 km^2), 3. Kumtag (22900 km^2), 4. Badain Jaran (44300 km^2), 5. Tengger (42700 km^2), 6. Ulan Buh (9900 km^2), 7. Hobq (16100 km^2), 8. Mu Us (32100 km^2), 9. Onqin Daga (21400 km^2), 10. Horqin (42300 km^2). Potential dust sources in China and Mongolia are divided into five sub-regions (A–E, hereafter northeastern sandy lands, near-CLP northern deserts, Gobi, Taklimakan and Tibetan deserts, respectively) for simplicity and two focused downwind deposition sites are marked as CLP(105–115°E, 33–37°N) and JS(130–138°E, 38–42°N). The lines marked as N36, N39 and N42 indicate the latitude lines of 36°N, 39°N and 42°N, respectively.

removed. In other words, once a potential source region is removed in the model domain, the resulted reductions in eolian dust emission and deposition fluxes, if any, represent the contributions from this source. For simplicity, the removed desert region in each experiment is entirely replaced by short grass, which is a typical land cover in northwestern China. This replacement could have changed the land surface properties in the original desert regions and affected local atmospheric conditions, and may eventually induce some uncertainties to the dust budget. However, these errors are quite local (not shown) and do not affect our discussions on the large-scale dust distributions. Thus, the definition above is used in our study to ignore the uncertainty.

3. Results and analyses

3.1. Model validation

The validity of our simulations is first examined by comparing the simulated aerosol optical depth (AOD) over East Asia with satellite-retrieved data (Multi-angle Imaging Spectro-radiometer (MISR), 550 nm, 2001–2009, available at: http://eosweb.larc.nasa.gov/PRODOCS/misr/table_misr.html), as shown in Fig. 2. It can be seen that the model can render the general pattern of the observed AOD, especially in northwestern China where mineral dust is the primary aerosol type. The maximal simulated AOD is clearly visible over the Taklimakan deserts, coincident with the observed data. However, the peak values of the simulated AOD are slightly higher than the MISR estimates in the source areas.

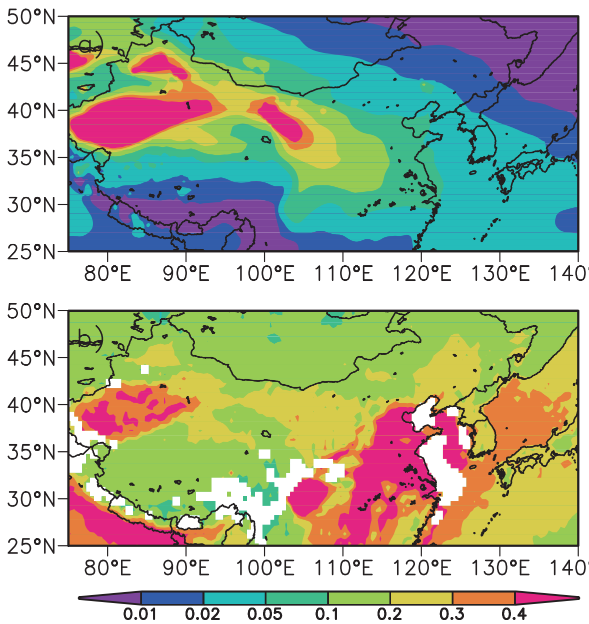

Fig. 2. Annual mean AOD (dust only) simulated with RegCM3 (a) and that (all aerosol types) retrieved from the MISR at the wavelength of 550 nm (b) over East Asia.

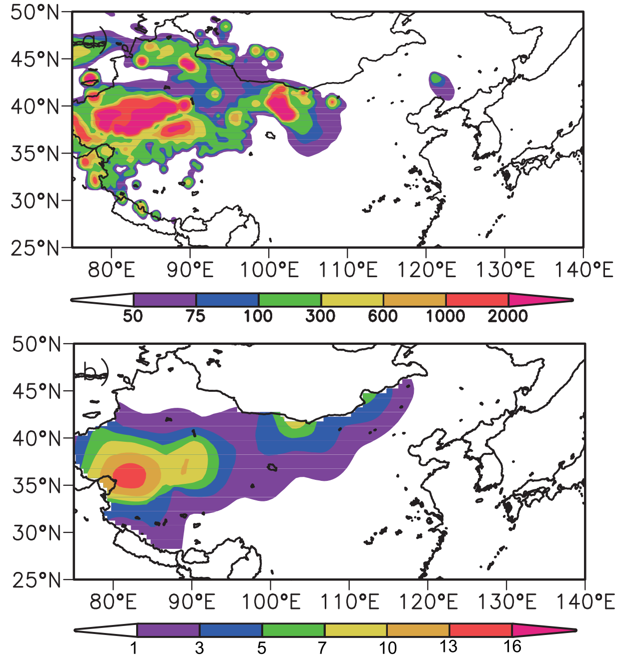

Fig. 3. Simulated annual surface dust concentrations larger than 50 μg m^{-3} (a) and station-observed annual-mean dust storms frequency in China for 1954–2007 (b).

On the other hand, the simulated AOD are smaller in the eastern China because our model does not include other aerosol types as presented in the MISA estimates, such as air pollution from major urban areas in this region.

The surface dust concentrations have high values mainly occurring around the Taklimakan and northern deserts, indicating that these near-source regions are mostly plagued by dust events and are in good agreement with the station-observed annual dust-storm high-frequency areas (Fig. 3). The simulated wind fields are also examined since it is of great importance for both dust generation and transport processes (Fig. 4). Our simulation can well reproduce the wind fields over East Asia, both for the near-surface and high altitudes. However, the simulated surface wind speeds are slightly larger especially over the Taklimakan deserts, which is probably the main reason for the overestimated AOD in northwestern source regions (Fig. 2).

A comparison of the simulated fine-grained dust MARs with the Dust Indicators and Records of Terrestrial and Marine Palaeoenvironments data set version 3 (DIRTMAP3, Maher and Kohfeld, 2009) also shows that their values are consistently within the same order of magnitude over the CLP (Fig. 5). Although the dust size ranges between simulated (less than 20 μm) and observed data (less than 10 μm) are not very consistent, we can still expect that the MARs are reproduced quite well. In the JS, the simulated MAR corresponds well with the observed value, however, the spatial pattern over the JS cannot be well validated as only the measurements at one site are available in the DIRTMAP3 database. Results above show that the model

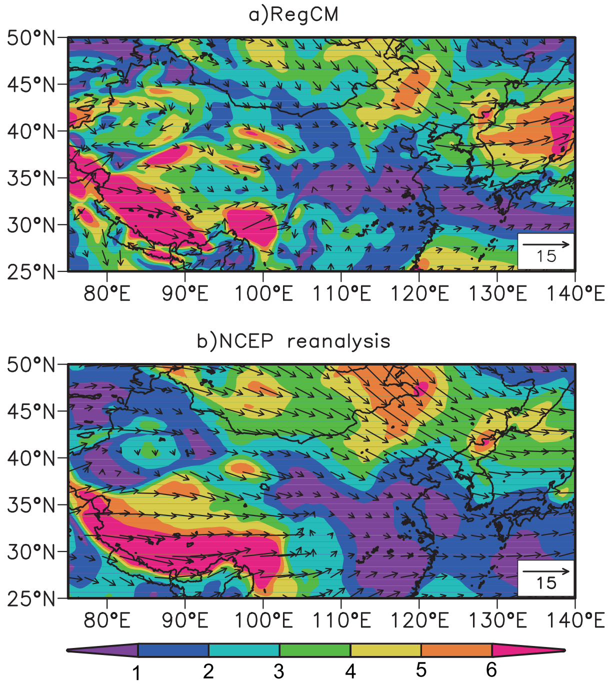

Fig. 4. Mean 850 hPa wind vectors (arrow, m s^{-1}) and 1000 hPa surface wind velocity (contour, m s^{-1}) in spring (1994–1998) from RegCM3 simulation (a) and NCEP reanalysis (b).

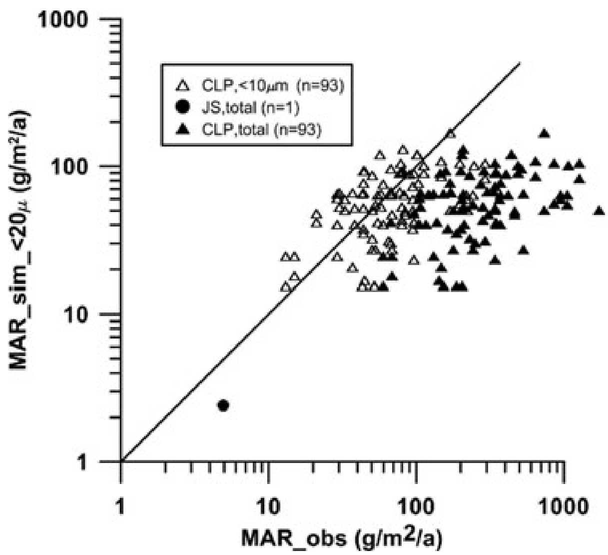

Fig. 5. Comparisons between simulated MARs and DIRTMAP3 data over East Asian regions. Sites in Chinese Loess Plateau and Japan Sea are respectively marked as triangles and circles. Note that the simulated MARs only covers the particles less than 20 μm, while the observed MARs is respectively for the entire dust sizes (solid triangles) and for those less than 10 μm (empty triangles).

can capture the dust cycle quite well, including the emission, atmospheric column loading and deposition across East Asia. This allows us to further quantify the relative contributions from these source regions in the following.

Table 1. The annual dust emission over China and Mongolia and contribution and emission efficiency for each source

	Emission (Tg)	Percentage (%)	Efficiency (10^{-4} Tg km^{-2})
A	89	5.2	3.5
B	308	17.9	8.9
C	178	10.4	1.6
D	1043	60.7	9.9
E	99	5.8	1.3
Total	1717	100	4.8

3.2. *Contributions of eolian dust from each source*

The total annual emission amount and percentage for each source region in East Asia are shown in Table 1. A total dust emission of 1717 Tg is simulated from the Chinese and Mongolian deserts, close to the estimate of Zhang et al. (1997). The largest dust source in East Asia is the Taklimakan deserts (Region D), occupying more than one-half of the total emission of the sources considered. Both high surface wind speeds and wide source areas facilitate the dust mobilization in this region. The northern deserts (Region B) and Gobi deserts (Region C) are also significant contributors of mineral dust, which account for 17.9% and 10.4%, respectively. Although the widest source area is found in Gobi region, the corresponding emission represents a less important contribution since its different soil texture has significantly suppressed the local mobilization. Dust sources on the Tibetan Plateau (Region E) merely play a minor role (5.8%) in the emission because of their high elevations and snow cover during the emission season. However, Tibetan dust might be still of significance in modern climate since it can be easily mobilized into the upper troposphere and transported for long distances. The dust emission from the northeastern sandy lands (Region A) is the smallest among the five sources (5.2%).

The dust deposition flux over East Asia is shown in Fig. 6 with peak values close to the source regions, especially in northwestern China. Eolian dust from these sources is mainly transported eastward and covers the eastern China, the Korean Peninsula, Japan and the nearby marine regions (Fig. 6a). As the two largest dust sources within China, the Taklimakan and near-CLP deserts dominate the dust accumulation rates in most parts of East Asia (Fig. 6c,e). In our simulations, eolian dust from the Taklimakan deserts tends to be transported further northward, hence primarily controlling the deposition fluxes over northwestern China and northern Mongolia, even affecting regions much further north. Meanwhile, in most parts of the eastern China, dust deposits are usually originated from near-CLP deserts, indicating their crucial role in regional distributions of mineral dust in China. Dust from the Gobi deserts and Tibetan Plateau can merely affect local depositions and provide limited contributions for

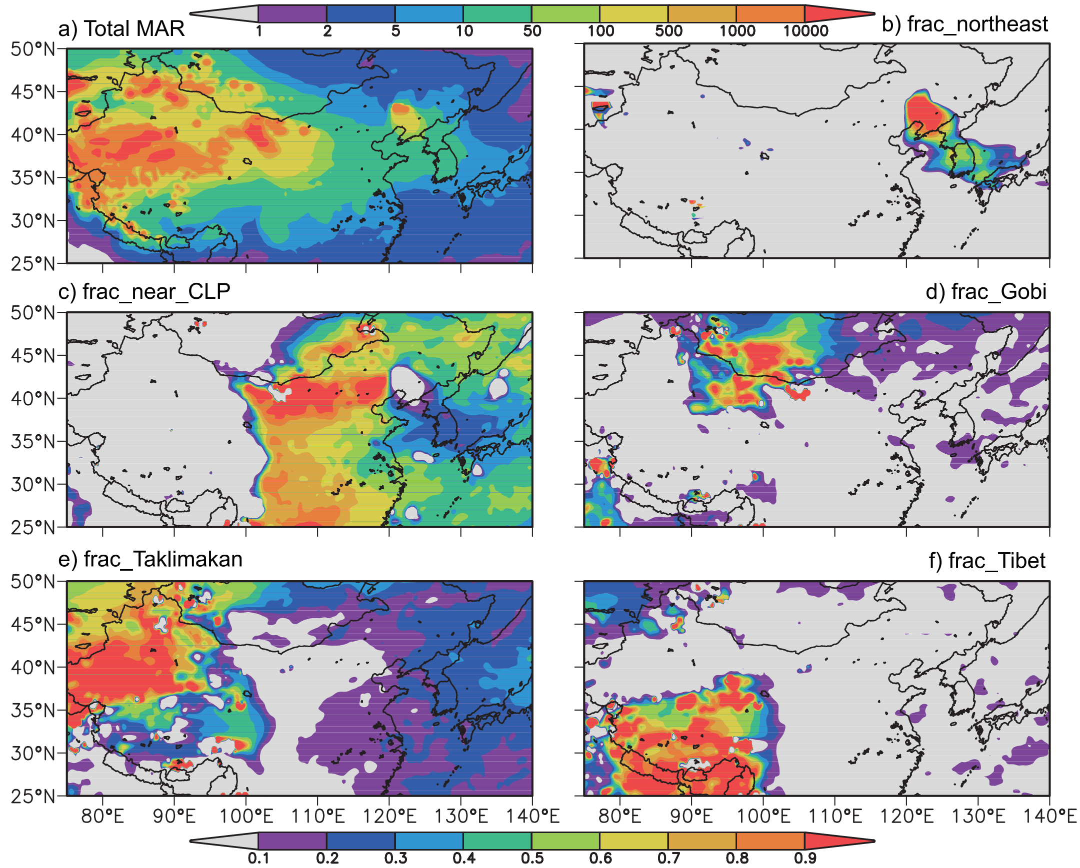

Fig. 6. The simulated MARs over East Asia (a, g/m^2/a) and the percentage contributions to the MARs from each source: Northeastern sandy regions (b); Near-Chinese Loess Platau deserts (c); Gobi (d); Taklimakan (e) and Tibet an Plateau (f). See the text for the percentage contributions.

other near-source regions due to their relatively small emissions (Fig. 6d,f). Although the northeastern sandy lands are found to be the smallest source in East Asia, they still can significantly affect the eolian dust deposits over the northeastern Asia due to their much close proximity (Fig. 6b).

The relative contributions from each dust source in the eolian deposits in the two focus regions (CLP and JS) are shown in Table 2. Our simulations indicate that more than 90% of the eolian dust in the CLP is originated from the near-CLP and Gobi deserts. In spite of its huge emission (60.7%), Taklimakan deserts only account for a minor fraction (6.4%) of the dust deposition fluxes. On the other hand, the contributions from the northeastern sandy lands and Tibet can be virtually neglected. Contrarily, the relative contributions from these sources to the JS deposits are distinctly different because this region is quite far away from the inland deserts. The near-CLP, Taklimakan deserts and northeastern sandy lands become the three largest sources for the JS marine deposits, accounting for about 34.2%, 29.2% and 24.3% of the total, respectively. The increasing fraction of Taklimakan deserts indicates that in the marine regions far enough from dust sources, the relative contributions of different sources are more inclined to be impacted by their emission amounts. The northeastern sandy areas understandably play a comparable role with the other large dust sources which is profited from their close proximity, consistent with Nagashima et al. (2007). The relative contributions from each source in the atmospheric column loadings are in good agreement with those of the deposition fluxes, implying that the atmospheric dust concentration and its provenance in the deposition regions can be

Table 2. Percentage contributions for each dust source to the dust deposition flux and atmospheric dust loading over CLP and JS. The mean values for total deposition flux and loading are also shown for reference

	Deposition CLP	JS	Loading CLP	JS
A	0.0%	24.3%	0.0%	15.4%
B	83.7%	34.2%	80.9%	50.5%
C	8.7%	9.7%	6.5%	7.7%
D	6.4%	29.2%	10.3%	23.0%
E	1.2%	2.6%	2.3%	3.4%
Total	61.8 mg m^{-2} d^{-1}	4.8 mg m^{-2} d^{-1}	88.1 mg m^{-2}	11.7 mg m^{-2}

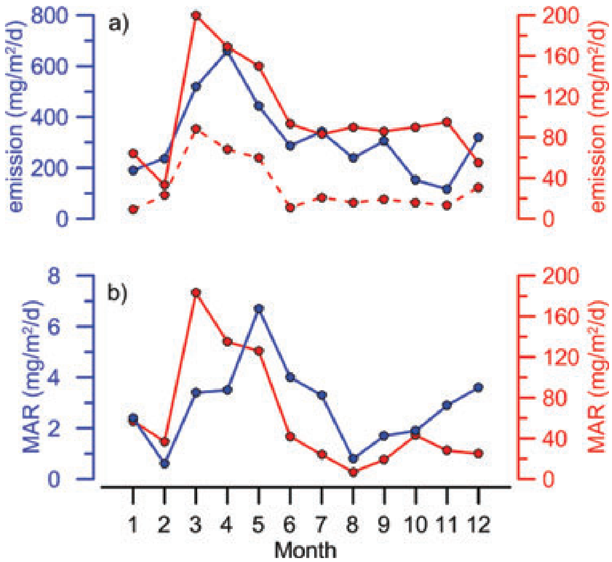

Fig. 7. (a) Monthly dust emission fluxes from three dust sources: Taklimakan (blue solid), near-Chinese Loess Plateau deserts (red solid) and northeastern sandy lands (red dashed). (b) Monthly MARs in the downwind Chinese Loess Plateau (red) and Japan Sea (blue).

reasonably deduced by the properties of the eolian deposits in these locations, which has been widely used in the observational studies (e.g. Sun, 2002; Lambert et al., 2008). However, our focus is mainly to quantify the relative contributions from East Asian deserts and actually we cannot exclude the potential contribution in the eolian deposits over CLP and JS from central Asian deserts which are not considered in our study.

The seasonal variability in the emission and deposition fluxes is shown in Fig. 7. For all the dust sources in East Asia, dust mobilization primarily occurs during spring, consistent with modern observations (Zhou and Zhang, 2003). However, the Taklimakan deserts have large emission amounts in other seasons as well, which are even greater than some other sources in their peak emission seasons. This causes northwestern China to suffer from dust events nearly all year around. The dust deposition over the near-source CLP is concentrated simultaneously during the emission season; while in the JS, the deposition reaches its peak at a later time. Another maximum deposition flux occurs at the end of the year when the increased contributions from Taklimakan and northeastern deserts may help to transport more dust to the region of JS.

Distinct differences are found in the particle size distributions of the eolian deposits at different locations (Table 3). Particle size distributions respond closely to the distance away from the sources: the longer the distance, the smaller the particles in the atmosphere. In the far-away JS, the finer modes no doubt dominate the total depositions and the particles larger than 5 μm only occupy a very small fraction of 2.8%. However, due to the very short distances between the CLP and the dust sources, the larger particles (larger than 5 μm) account for almost three-fifths of total flux, primarily coming from the near-CLP deserts (89.8%). This might explain why in our simulations the dust from near-CLP deserts nearly dominates the eolian deposits in the CLP. The second peak (21.0%) occurs in the finer mode (less than 1 μm) and a majority of these finer particles is originated from the Taklimakan deserts.

Table 3. The mass percentages for each bin in the eolian sediments and the corresponding contributions of 5 source regions in each bin over CLP and JS

Region		0.01–1.0 μm	1.0–2.5 μm	2.5–5.0 μm	5.0–20.0 μm
CLP	Total	21.0%	9.0%	11.9%	58.1%
	A	0.0%	0.0%	0.0%	0.0%
	B	70.8%	81.5%	75.0%	89.8%
	C	14.3%	10.6%	11.4%	8.3%
	D	13.9%	6.5%	10.5%	1.9%
	E	1.0%	1.4%	3.1%	0.0%
JS	Total	72.2%	11.1%	13.9%	2.8%
	A	9.2%	28.8%	23.4%	34.3%
	B	28.6%	36.5%	31.7%	35.7%
	C	7.7%	5.9%	13.5%	10.0%
	D	48.5%	25.3%	24.7%	6.7%
	E	6.0%	3.5%	6.7%	13.3%

The proportions of the dry/wet deposition processes also vary in the two focused regions (Fig. 8). In the JS (Fig. 8a), the wet deposition process is the dominant mechanism of dust removal (80–90% of the total removal) all year round due to the large fraction of relatively fine particles that are difficult to resettle

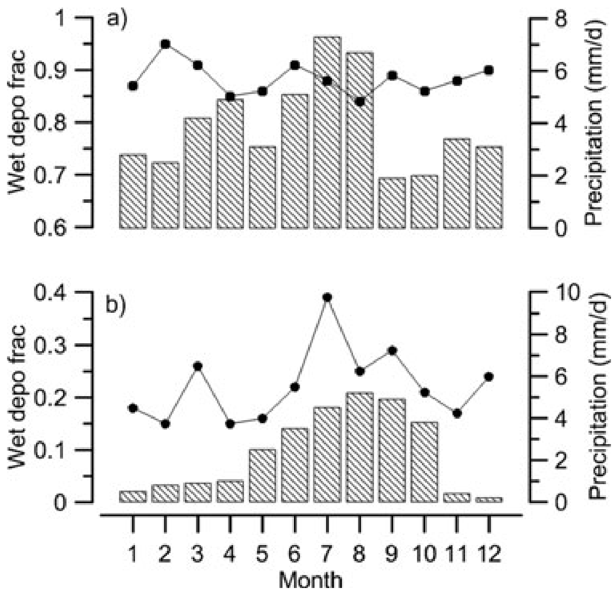

Fig. 8. Monthly contributions (%, line chart) of wet deposition relative to the total deposition and the precipitation rate (mm/d, bar chart) over Japan Sea (a) and Chinese Loess Plateau (b).

gravitationally and can reside in the atmosphere for a long time. In spite of its obvious seasonality of precipitation, the percentage contribution from wet deposition process does not vary so much, indicating that it is not very sensitive to the precipitation as a result of small atmospheric loading in this region (Table 2). On the other hand, the coarser particles are more likely to be deposited through the dry deposition process over the CLP. As shown in Fig. 8b, the relative contribution from wet deposition is dependent on the precipitation. Furthermore, it is very likely that high frequencies of rainfall events are actually responsible for the effective wet deposition removal of dust.

The transport paths of the eolian dust are further examined, focusing on the two most important sources (the Taklimakan and near-CLP deserts) for simplicity. When all dust sources are considered, dust from inland deserts moves upward and travels eastward (Fig. 9a). Two maximum centres are specified, which are respectively corresponding to the Taklimakan and near-CLP deserts. The dust plumes for long-distance delivery are mainly concentrated at the lower and middle troposphere but with a significant portion reaching up to the upper troposphere. For the near-CLP deserts, the eolian dust is restricted to the levels below 400 hPa and delivers primarily in the lower troposphere (Fig. 9b). On the other hand, the dust residing in the upper troposphere is mainly originated from the Taklimakan deserts and tends to be transported in the higher levels than that from the near-CLP deserts (Fig. 9c) due to the stronger local vertical convection (Fig. 9a). We use the isobaric levels of 850 hPa and 500 hPa to represent the lower and middle tropospheric dust concentrations and horizontal wind fields in spring, the season of major dust events in East Asia (Fig. 10). In spring, the East Asian winter monsoon system still dominates the regional circulation in the northern China and then controls the leading delivery direction in the northern China. Under the action of the northwesterly winds, the eolian dust from both sources travels southeastward (Fig. 10a,b), bringing most eolian dust in the downwind regions of East Asia. Meanwhile in the middle troposphere, the eolian dust is transported eastward caused by the predominant westerly winds (Fig. 10c,d). Only a limited amount of the near-CLP dust

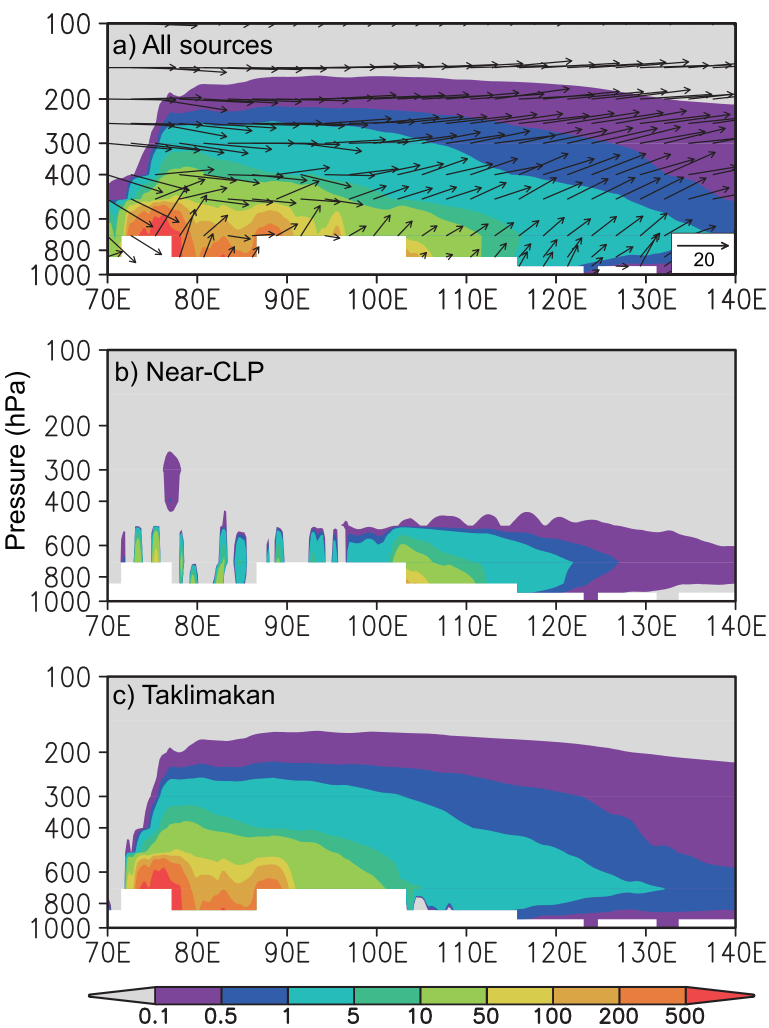

Fig. 9. The simulated longitude-height cross section of vertical wind field (a, Pa s^{-1}) and dust concentration ($\mu g\ m^{-3}$) averaged for 36–50°N for eolian dust originated from (a) all sources; (b) near-Chinese Loess Plateau deserts; (c) Taklimakan deserts.

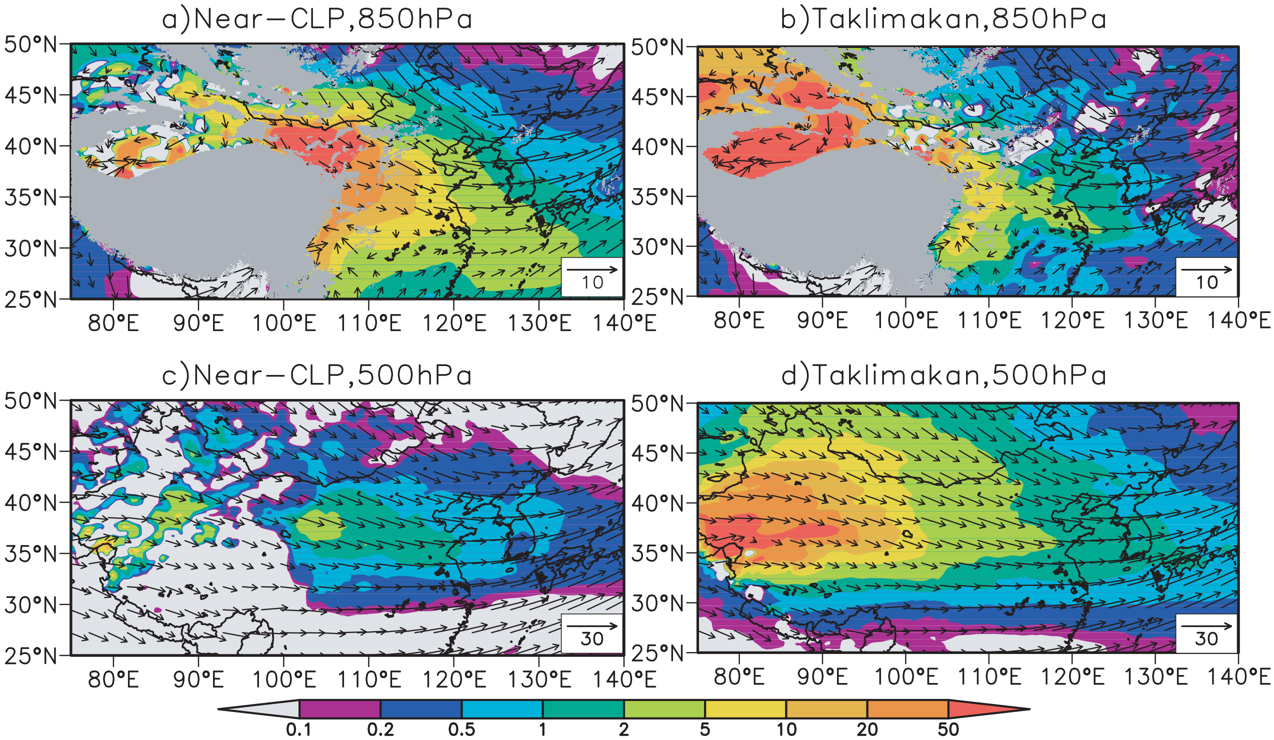

Fig. 10. The 850 hPa (top panel) and 500 hPa (bottom panel) horizontal wind vectors (m s^{-1}) and dust concentration (μg m^{-3}) distributions for eolian dust from near-Chinese Loess Plateau (a,c) and Taklimakan (b,d) deserts in spring.

can move up to this level and, hence, nearly all high-level dust can be considered to be generated from Taklimakan (Fig. 10d). The finer dust in the upper levels tends to deliver a longer distance and this explains why the Taklimakan dust plays a more significant role in the eolian deposits in the far-away JS. The significance of the contribution from the Taklimakan deserts increases with distance. Therefore, it is reasonable to extrapolate that in the further-away North Pacific, the fraction of the Taklimakan dust contribution likely become even more significant.

3.3. Discussions

From the above simulations, Taklimakan deserts, Near-CLP northern deserts and Gobi deserts are considered as three major dust sources in East Asia, in agreement with former studies (Zhang et al., 1997, 2003). However, our estimates of their contributions (60.7%, 17.9% and 10.4%, respectively) are slightly different. Zhang et al. (2003) proposed that these three sources share similar proportions with a total fraction of about 70% in the Asian dust emission. Comparatively, our results indicate a more important role from Taklimakan deserts than any other source areas, which is mainly profited from our new soil textures, strong surface wind speeds and large source areas over this region. Larger particle sizes could decrease the binding energy and facilitate the surface collision and particle release (Alfaro et al., 1998). This remarkable contribution of Taklimakan is also visibly detected by modern observations showing that large areas are covered by higher AODs over Taklimakan compared to those in Gobi and near-CLP deserts (Fig. 2b). Hence, our simulated results are more likely reasonable that Taklimakan deserts could be the largest dust source in East Asia.

Different size distributions of dust particles over deposition regions are indicated in our simulations, which is ascribed to different distances from dust sources. In CLP deposits, the simulated peak is at the bin of 5.0–20.0 μm, quite similar with the observation studies in or near source regions (Gao et al., 1997; Zhang et al., 1998). But the simulated size distributions are probably smaller over far-away JS. In the observations around JS or East China Sea, the size bin with maximum dust concentration is usually located in the ranges of several microns (Fu et al., 2004; Hsu et al., 2009; Park et al., 2004). However, a largest mass fraction is simulated in the size bin of 0.01–1.0 μm. This difference is mainly due to the overestimation of dry deposition removal in the model for relatively larger particles (Zhang et al., 2009). Because of the limited bins in the model and their mismatched divisions with observation data, it is difficult for us to directly compare the dust sizes between simulations and observations. Thus, further validation on the model's ability to simulate dust sizes is still required in the future.

In previous studies (Sun, 2004), a remarkable bi-mode grain-size distribution is widely observed in the eolian sediments in the northern China. The coarse component, which is usually

20–70 μm in diameter, is accepted to be from adjoining dust sources since these particles are too large to be delivered for long distances. However, the provenance of the fine component is still controversial. Our study focusing on the fine component confirms a dominate role of the adjoining deserts (near-CLP and Gobi) in the dust deposition over CLP, exceeding a fraction of 90%, which is consistent with some tracer studies (Sun, 2002; Sun et al., 2008). In spite of being the largest dust source, Taklimakan deserts merely account for about 6.4% of the total deposition flux in the CLP. Due to short distances, the eolian dust from the adjoining deserts dominates the deposition fluxes of the coarser particles (5–20 μm in our model) while Taklimakan deserts only contribute to the component of the finer particles (0.01–1 μm). If the factor is considered that our model might underestimate the fractions of larger particles in the eolian deposits, the contributions of Taklimakan deserts in the larger size bins would further increase.

The hypothesis regarding the transport mechanisms of the Chinese eolian dust (Sun, 2004) also gains supports from our simulations. Our simulations indicates that dust particles from the near-CLP deserts are mainly delivered by the low-level northwesterly winter monsoon system in spring and only a very small portion of the particles can move into the upper atmosphere. In the regions without the control of winter monsoon system (i.e. the Taklimakan deserts), finer particles from Taklimakan deserts are raised into the upper atmosphere and then transported via westerly winds. However, a dominant role of northwesterly system is still found in the fine-grained eolian deposits of CLP. This pathway of the Taklimakan dust transport plays an important role in the marine sediments in the JS, and possibly also in the North Pacific. Nearly one-half of the finer particles in the JS sediments are carried from Taklimakan. One important point is that not all finer particles can be raised into the upper atmosphere. A comparable proportion of them are carried by low-level westerly winds and reaches the regions where the winter monsoon system dominates. In the JS sediments, the contribution from the Taklimakan deserts has been significantly increased. Thus, the marine deposition fluxes can reflect the inland aridity at a broad spatial scale beyond merely the local region.

4. Conclusions

The CLP located in northern China provides an excellent experimentation ground for understanding the modern- and palaeoclimatic processes associated with eolian dust cycle in East Asia. The provenance of fine-grained eolian dust over the CLP and the further-away JS are simulated by using a regional climate model in this study. Our results suggest that the Taklimakan, near-CLP and Gobi deserts are the three primary dust sources for East Asia, accounting for 89% of the total dust emission from all the sources in China and Mongolia.

In the CLP, the eolian dust is mainly originated from the near-CLP northern deserts (83.7%) and the contribution of the Taklimakan deserts is very limited (6.4%), while in the further-away JS, the fraction of the Taklimakan dust has been significantly increased and the northeastern sandy lands also play a comparable role in the eolian deposits due to close proximity.

Eolian dust from the near-CLP deserts tends to be delivered in the lower-level atmosphere as a result of the dominant East Asian winter monsoon system. Due to the effect of strong local convection, a large proportion of the eolian dust from the Taklimakan deserts is transported in the middle and upper troposphere by the predominant westerly winds for a long-distance delivery. As the distances to the sources increase, the fractions of the finer particles of the total deposition flux increase, together with the enhanced component from the Taklimakan deserts. Therefore, the Taklimakan deserts may be a significant contributor to the marine deposits as far as the North Pacific, if not even further.

In summary, our study provides useful information to distinguish the provenance of the Chinese loess from a model perspective that nearly all fine eolian dust over the CLP is found to be originated from the nearby deserts in the modern time, supporting the results of some of the tracer studies. However, our results may be model-dependent and only confined under modern boundary conditions and we can not simply extrapolate them to geological periods, such as the last glacial maximum. To fully understand the cycle processes of the Asian dust, hence, further effort is eagerly required both for the model and tracer communities.

5. Acknowledgments

We thank two anonymous reviewers for their constructive comments to improve the manuscript and Dr. Zhiyong Yin for the language editing. This work was jointly supported by the '973' Program (2011CB403406), Innovation Program of Chinese Academy of Sciences (KZCX2-EW-114), NSFC (40825008, 41075067).

References

Alfaro, S. C., Gaudichet, A., Gomes, L. and Maillé, M. 1998. Mineral aerosol production by wind erosion: aerosol particle sizes and binding energies. *Geophys. Res. Lett.* **25**, 991–994.

Alfaro, S. C. and Gomes, L. 2001. Modelling mineral aerosol production by wind erosion: emission intensities and aerosol size distributions in source areas. *J. Geophys. Res.* **106**(D16), 18075–18084.

An, Z. S. 2000. The history and variability of the East Asian paleomonsoon climate. *Quat. Sci. Rev.* **19**, 171–187.

Biscaye, P. E., Grousset, F. E., Revel, M., Van der Gaast, S., Zielinski, G. A. and co-authors. 1997. Asian provenance of glacial dust (stage 2) in the Greenland Ice Sheet Project 2 Ice Core, Summit, Greenland. *J. Geophys. Res.* **102**, 26 765–26 781.

Bory, A. J.-M., Biscaye, P. E. and Grousset, F. E. 2003. Two distinct seasonal Asian source regions for mineral dust depositedin Greenland (North GRIP). *Geophys. Res. Lett.* **30**, 1167, doi:10.1029/2002GL016446.

Cao, J. J., Lee, S. C., Zhang, X. Y., Chow, J. C., An, Z. S. and co-authors. 2005. Characterization of airborne carbonate over a site near Asian dust source regions during spring 2002 and its climatic and environmental significance. *J. Geophys. Res.* **110**, D03203, doi:10.1029/2004JD005244.

Chung, Y. S., Kim, H. S., Dulam, J. and Harris, J. 2003. On heavy dustfall observed with explosive sandstorms in Chongwon-Chongju, Korea in 2002. *Atmos. Environ.* **37**, 3425–3433.

Clarke, A. D., Shinozuka, Y., Kapustin, V. N., Howell, S., Huebert, B. and co-authors. 2004. Size distributions and mixtures of dust and black carbon aerosol in Asian outflow: physiochemistry and optical properties. *J. Geophys. Res.* **109**, D15S09, doi:10.1029/2003JD004378.

Delmonte, B., Petit, J. R. and Maggi, V. 2002. Glacial to Holocene implications of the new 27000-year dust record from the EPICA Dome C (East Antarctica) ice core. *Clim. Dyn.* **18**, 647–660.

Dickinson, R., Henderson-Sellers, A. and Kennedy, P. 1993. Biosphere atmosphere transfer scheme (bats) version 1e as coupled to the NCAR community climate model. Technical report, National Center for Atmospheric Research, 72 pp.

Duce, R., Liss, P. S., Merrill, J. T., Atlas, E. L. and Buat-Menard, P. 1991. The atmospheric input of trace species to the world ocean. *Global Biochem. Cycles* **5**, 193–259.

Fang, X. M., Han, Y. X., Ma, J., Song, L., Yang, S. and co-authors. 2004. Dust storms and loess accumulation on the Tibetan PlateauA case study of dust event on March 2003 in Lhasa. *Chin. Sci. Bull.* **49**, 953–960.

Fecan, F., Marticorena, B. and Bergametti, G. 1999. Parametrization of the increase of the aeolian erosion threshold wind friction velocity due to soil moisture for arid and semi-arid areas. *Ann. Geophys.* **17**, 149–157.

Fu, F. F., Watanabe, K., Yabuki, S. and Akagi, T. 2004. Seasonal characteristics of chemical compositions of the atmospheric aerosols collected in urban seaside area at Tokaimura, eastern central Japan. *J. Geophys. Res.* **109**, doi:10.1029/2004JD004712.

Gao, Y., Arimoto, R., Duce, R. A., Zhang, X. Y., Zhang, W. Y. and co-authors. 1997. Temporal and spatial distributions of dust and its deposition to the China Sea. *Tellus* **49B**, 172–189.

Giorgi, F. 1989. Two-dimensional simulations of possible mesoscale effects of nuclear war fires, I: Model description. *J. Geophys. Res.* **94**(D1), 1127–1144.

Giorgi, F. and Chameides, W. L. 1986. Rainout lifetimes of highly soluble aerosols and gases as inferred from simulations with a general circulation model. *J. Geophys. Res.* **91**(D13), 14367–14376.

Gong, S. L., Zhang, X. Y., Zhao, T. L., Zhang, X. B., Barrie, L. A. and co-authors. 2006. A Simulated Climatology of Asian Dust Aerosol and Its Trans-Pacific Transport. Part II: Interannual Variability and Climate Connections. *J. Clim.* **19**, 104–122.

Grell, G. A. 1993. Prognostic evaluation of assumptions used by cumulus parameterizations. *Mon. Weather Rev.* **121**, 764–787.

Holtslag, A., de Bruijn, E. and Pan, H. L. 1990. A high resolution air mass transformation model for short-range weather forecasting. *Mon. Weather Rev.* **118**, 1561–1575.

Hou, S. S., Yang, S. L., Sun, J. M. and Ding, Z. L. 2003. Oxygen isotope compositions of quartz grains (4–16 mm) from Chinese eolian deposits and their implications for provenance. *Sci. China Ser. D* **46**, 1003–1011.

Hseung, Y. 1996. *The Soil Atlas of China*. Cartographic Publ., Beijing.

Hsu, S.-C., Liu, S. C., Arimoto, R., Liu, T.-H., Huang, Y.-T. and co-authors. 2009. Dust deposition to the East China Sea and its biogeochemical implications. *J.Geophys. Res.* **114**, D15304, doi:10.1029/2008JD011223.

Kalnay, E., Kanamitsua, M., Kistlera, R., Collins, W., Deaven, D. and co-authors. 1996. The NCEP/NCAR 40-Year Reanalysis Project. *B. Am. Meteorol. Soc.* **77**, 437–471.

Kiehl, J., Hack, J., Bonan, G., Boville, B., Breigleb, B. and co-authors. 1996. Description of the NCAR community climate model (ccm3). Technical report, National Center for Atmospheric Research, 152 pp.

Lambert, F., Delmonte, B., Petit, J. R., Bigler, M., Kaufmann, P. R. and co-authors. 2008. Dust-climate couplings over the past 800,000 years from the EPICA Dome C ice core. *Nature* **452**, 616–619.

Li, F., Ginoux, P. and Ramaswamy, V. 2008. Distribution, transport and depositoin of mineral dust in the Southern Ocean and Antarctica: contributions of major sources. *J. Geophys. Res.* **113**, doi:10.1029/2007JD009190.

Liu, C. S., Masuda, A., Okada, A., Yabuki, S. and Fan, Z. 1994. Isotope geochemistry of Quaternary deposits from the arid lands in Northern China. *Earth Planet. Sci. Lett.,* **127**, 25–38.

Liu, T. S. 1985. *Loess and the Environment*. China Ocean, Beijing.

Loveland, T. R., Reed, B. C., Brown, J. F., Ohlen, D. O., Zhu, J. and co-authors. 2000. Development of a global land cover characteristics database and IGBP DISCover from 1-km AVHRR data. *Int. J. Remote Sens.* **21**, 1303–1330.

Luo, C., Mahowald, N. and Corral, J. 2003. Sensitivity study of meteorological parameters on mineral aerosol mobilization, transport and idstribution. *J. Geophys. Res.* **108**, 4447, 10.1029/2003JD0003483.

Maher, B. A. and Kohfeld, K. 2009. 'DIRTMAP' Version 3, LGM and late Holocene Aeolian Fluxes from Ice Cores, Marine Sediment Traps, Marine Sediments and Loess Deposits. Available at: http://www.lec.lancs.ac.uk/dirtmap3. Accessed on March 2011.

Marticorena, B. and Bergametti, G. 1995. Modeling the atmospheric dust cycle, I, Design of soil-soilderived dust emission scheme. *J. Geophys. Res.* **100**(D8), 16415–16430.

Miller, R., Tegen, I. and Perlwitz, J. 2004. Surface radiative forcing by soil dust aerosols and the hydrologic cycle. *J. Geophys. Res.* **109**, D04203, doi:10.1029/2003JD004085.

Nagashima, K., Tada, R., Tani, A., Toyoda, S., Sun, Y. B. and co-authors. 2007. Contribution of aeolian dust in Japan Sea sediments estimated from ESR signal intensity and crystallinity of quartz. *Geochem. Geophys. Geosyst.* **8**, Q02Q04, doi:10.1029/2006GC001364.

Nakano, T., Yokoo, Y., Nishikawa, M. and Koyanagi, H. 2004. Regional Sr-Nd isotopic ratios of soil minerals in northern China as Asian dust fingerprints. *Atmos. Environ.* **38**, 3061–3067.

Pal, J. S., Giorgi, F., Bi, X., Elguindi, N., Solmon, F. and co-authors. 2007. Regional climate modeling for the developing world: The ICTP RegCM3 and RegCNET. *B. Am. Meteorol. Soc.* **88**(9), 1395–1409.

Pal, J. S., Small, E. E. and Eltahir, E. A. B. 2000. Simulation of regional scale water and energy budgets: representation of subgrid cloud and precipitation processes within RegCM. *J. Geophys. Res.* **105**(D24), 29 579–29 594.

Park, S. H., Song, C. B., Kim, M. C., Kwon, S. B. and Lee, K. W. 2004. Study on size distribution of total aerosol and water-soluble ions during an Asian dust storm event at Jeju Island, Korea. *Environ. Monit. Assess.* **93**, 157–183.

Porter, S. C. and An, Z. 1995. Correlation between climate events in the North Atlantic and China during the last glaciations. *Nature* **375**, 305–308.

Rea, D. K., Snoeckx, H. and Joseph, L. P. 1998. Late Cenozoic aeolian deposition in the north Pacific: asian drying, Tibetan uplift, and cooling of the Northern Hemisphere. *Paleoceanography* **13**, 215–224.

Reynolds, R. W., Rayner, N. A., Smith, T. M., Stokes, D. C. and Wang, W. 2002. An improved in situ and satellite SST analysis for climate. *J. Clim.* **15**, 1609–1625.

Rosenfeld, D. 2000. Suppression of rain and snow by urban and industrial air pollution. *Science* **287**, 1793–1796.

Solmon, F., Giorgi, F. and Liousse, C. 2006. Aerosol modeling for regional climate studies: application to anthropogenic particles and evaluation over a European/African domain. *Tellus* **58B**, 51–72.

Sun, D. H. 2004. Monsoon and westerly circulation changes recorded in the Late Cenozoic aeolian sequences of Northern China. *Global Planet. Change* **41**, 63–80.

Sun, J. M. 2002. Provenance of loess material and formation of loess deposits on the Chinese Loess Plateau. *Earth Planet. Sci. Lett.* **203**, 845–859.

Sun, J. M., Zhang, M. Y. and Liu, T. S. 2001. Spatial and temporal characteristics of dust storms in China and its surrounding regions 1960 1999 Relations to source area and climate. *J. Geophys. Res.* **106**, 18 325–18 333.

Sun, Y. B. and An, Z. S. 2002. History and variability of the Asian interior aridity recorded by eolian flux in the Chinese Loess Plateau during the past 7 Ma. *Sci. China Ser. D* **45**(5), 420–429.

Sun, Y. B., Tada, R., Chen, J., Liu, Q. S., Toyoda, S. and co-authors. 2008. Tracing the provenance of fine-grained dust deposited on the central Chinese Loess Plateau. *Geophys. Res. Lett.* **35**, doi:10.1029/2007GL031672.

Tanaka, T. and Chiba, M. 2006. A numerical study of the contributions of dust source regions to the global dust budget. *Global Planet. Change* **52**, 88–104.

Tegen, I. and Lacis, A. 1996. Modeling of particle size distribution and its influence on the radiative properties of mineral dust aerosol. *J. Geophys. Res.* **101**, 19 237–19 244.

Torii, M., Lee, T. Q., Fukuma, K., Mishima, T., Yamazaki, T. and co-authors. 2001. Mineral magnetic study of the Taklimakan desert sands and its relevance to the Chinese loess. *Geophys. J. Int.* **146**, 416–424.

Wang, Y. Q., Zhang, X. Y., Arimoto, R., Cao, J. J. and Shen, Z. X. 2005. Characteristics of carbonate content and carbon and oxygen isotopic composition of northern China soil and dust aerosol and its application to tracing dust sources. *Atmos. Environ.* **39**, 2631–2642.

Zakey, A. S., Solmon, F. and Giorgi, F. 2006. Implementation and testing of a desert dust module in a regional climate model. *Atmos. Chem. Phys.* **6**, 4687–4704.

Zhang, D. F., Zakey, A. S., Gao, X. J., Giorgi, F. and Solmon, F. 2009. Simulation of dust aerosol and its regional feedbacks over East Asia using a regional climate model. *Atmos. Chem. Phys.* **9**, 1095–1110.

Zhang, X. Y., Arimoto, R. and An Z. S. 1997. Dust emission from Chinese desert sources linked to variations in atmospheric circulation. *J. Geophys. Res.* **102** (D23), 28 041–28 047.

Zhang, X. Y., Arimoto, R., Zhu, G. H., Chen, T. and Zhang, G. Y. 1998. Concentration, size-distribution and deposition of mineral aerosol over Chinese desert regions. *Tellus* **50B**, 317–331.

Zhang, X. Y., Gong, S. L., Zhao, T. L., Arimoto, R., Wang, Y. Q. and co-authors. 2003. Sources of Asian dust and role of climate change versus desertification in Asian dust emission. *Geophys. Res. Lett.* **30**, 2272, doi:10.1029/2003GL018206.

Zhang, X. Y., Zhang, G. Y., Zhu, G. H., Zhang, D. E., An, Z. S. and co-authors. 1996. Elemental tracers for Chinese source dust. *Sci. China (Series D)* **395**, 512–521.

Zhou, Z. J. and Zhang, G. C. 2003. Typical severe dust storms in northern China during 1954–2002. *Chin. Sci. Bull.* **48**, 2366–2370.